DOI: 10.1002/ejic.200501019

Boron–Nitrogen Adducts of 1,3,5-Triaza-7-phosphaadamantane (PTA): Synthesis, Reactivity, and Molecular Structure

Brian J. Frost,*[a] Charles A. Mebi,[a] and Phillip W. Gingrich[a]

Keywords: Borane adducts / Boroxine / N,P ligands / Coordination modes / Structure elucidation

Addition of BH_3 to 1,3,5-triaza-7-phosphaadamantane (PTA) leads to the formation of the first coordination complex of PTA in which a nitrogen and not the phosphorus of PTA is involved in the bonding. Multinuclear NMR spectroscopy, X-ray crystallography, and computational chemistry are utilized in the characterization of the products. Crystal structures of PTA–BH_3 (**1**) and O=PTA–BH_3 (**2**) adducts are described. In addition a coordination polymer, $[CpRu(PTA)_2Cl(Ph_3B_3O_3)]_n$ (**3**), resulting from Lewis acid–base adduct formation between the PTA ligands of $CpRu(PTA)_2Cl$ and the product of the cyclocondensation of phenylboronic acid is described. The polymeric compound **3** was also characterized by X-ray crystallography.

Introduction

The coordination chemistry and catalytic activity of metal complexes containing aminophosphane ligands has been explored extensively in recent years.[1] Much of the interest in this class of ligand arises from the variety of coordination modes possible (i.e. *N*-bound, *P*-bound, or N–P chelate). Particularly important for catalytic applications is the hemilabile nature of the hard nitrogen donor.[2] Our group,[3–5] and others,[6] have been interested in the chemistry of the heterocyclic phosphane 1,3,5-triaza-7-phosphaadamantane (PTA), which was first synthesized by Daigle in the 1970s (Figure 1).[7,8] The attractive properties of PTA are its resistance to oxidation, small size, strong binding ability, and water solubility. Although PTA is an aminophosphane, the adamantane-like structure excludes the possibility of P–N chelate formation. PTA coordinates to metal atoms through the phosphorus atom, with only one known example of a PTA complex containing a nitrogen–metal dative bond; a polymeric structure formed through the coordination of a nitrogen of a ruthenium-bound PTA ligand to silver.[9] Because metals preferentially bind to the phosphorus of PTA, the amine functionalities of PTA are the preferred site of alkylation and protonation.[7,10] We have been interested in the coordination chemistry of PTA and, specifically, why transition metals bind to the phosphorus site and other Lewis acids, such as H^+ and R^+, bind preferentially, although not exclusively, to the nitrogen sites. Methylation of PTA with MeI leads to *N*-methylated PTA (PTA-Me) with a small amount, $< 5\%$, of the *P*-methylated PTA (Me-PTA).[10,11] The synthesis of *P*-alkylated PTA derivatives may be accomplished by starting with phosphane sources such as R-PH_2 or $P(CH_2OH)_3$, Scheme 1.[12,13]

Figure 1. PTA.

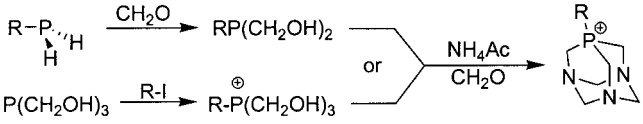

Scheme 1.

Herein we present experimental and theoretical data on the addition of BH_3 to PTA and O=PTA, affording the first coordination complex of PTA involving only nitrogen coordination. Also described is an extended polymeric structure, $[CpRu(PTA)_2Cl(Ph_3B_3O_3)]_n$, held together by B–N coordination of a PTA nitrogen to triphenylboroxine.

Results and Discussion

BH_3 complexes of PTA and O=PTA, **1** and **2** respectively, have been synthesized in good yield by addition of BH_3–THF to PTA or O=PTA. In both cases, addition of BH_3 leads to the formation of a N–B coordination complex, Scheme 2. As it is not surprising that such complexes are formed, compound **1** is, to the best of our knowledge, the first example of a coordination complex of PTA in which only nitrogen of PTA is involved in bonding. Peruzzini et al. recently reported the first example of a coordination

[a] Department of Chemistry, University of Nevada, Reno, NV 89557, USA
Fax: +1-775-784-6804
E-mail: Frost@chem.unr.edu

complex involving binding of a nitrogen of PTA to another metal;[9] in this case the phosphorus of PTA is already coordinated to ruthenium. There are still no examples in the literature of a nitrogen-bound PTA–metal complex in which the phosphorus is not also coordinated to a metal.

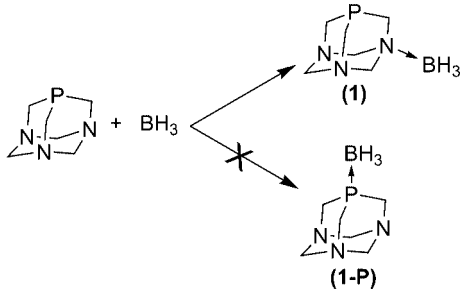

Scheme 2.

The site of BH_3 binding has been determined by: X-ray crystallography, computational chemistry, IR spectroscopy, ^1H, ^{31}P, and ^{11}B NMR spectroscopy, all of which indicate that addition of BH_3 results in preferential B–N and *not* B–P bond formation. No evidence of P–B bond formation was observed by any spectroscopic method including ^{11}B or ^{31}P NMR spectroscopy.[14,15]

Addition of BH_3 to PTA or O=PTA results in a slight shift of the ^{31}P NMR resonances with respect to PTA and O=PTA. The complexes **1** and **2** exhibit ^{31}P NMR resonances at –88.4 and –9.8 ppm, respectively, compared to –98.3 and –2.5 ppm for PTA and O=PTA.[7,8] These shift values are similar to those observed for the methylation of PTA; $PTA(Me)^+$ exhibits a ^{31}P NMR resonance at –86.1 ppm.[6] The ^{11}B NMR spectra of **1** and **2** were obtained with resonances at –10.8 ppm for **1** (quartet, $^1J_{BH}$ = 98 Hz) and –12.2 ppm for **2** (quartet, $^1J_{BH}$ = 95 Hz). These values compare well with other ^{11}B chemical shifts of other $H_3B–NR_3$ compounds. For example, the ^{11}B NMR chemical shift of the borane adducts of 1,3,5-trimethyl-1,3,5-triazacyclohexane[16] and 3,5-dimethyl-1,3,5-thiadiazacyclohexane[17] were found to be –12.6 ppm (q, $^1J_{BH}$ = 96 Hz) and –11.1 ppm (q, $^1J_{BH}$ = 97 Hz), respectively.

The solid-state structures of **1** and **2** were determined by X-ray crystallography. Crystals suitable for X-ray analysis were obtained by slow diffusion of hexanes into a THF solution of the complex at room temperature over 3 days.

Structure of $PTA–BH_3$ (1)

A thermal ellipsoid representation of complex **1** is depicted in Figure 2, along with the atomic numbering scheme. Selected bond lengths and angles may be found in Table 1. The overall structure including bond lengths and angles is practically identical to that of PTA. Noteworthy is that the B–N bond length [1.58(2) Å] in **1** is similar to that found in the DABCO adduct, $N(CH_2CH_2)_3N–BH_3$ (B–N = 1.598 Å),[18] and is slightly shorter than the B–N bond in the hexamethylenetetramine–borane adduct [B–N = 1.661(7) Å].[19] Also of note is that the (B)N–C(N) bond length, 1.505(9) Å, is longer than the other N–C(N) bond lengths, 1.458(9) Å, consistent with other PTA complexes

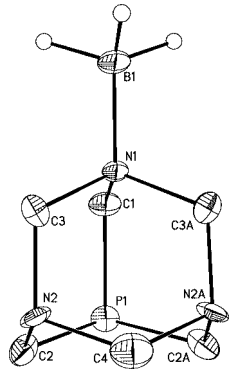

Figure 2. Thermal ellipsoid plot of $PTA–BH_3$ showing the atomic numbering scheme; hydrogen atoms have been omitted for clarity; thermal ellipsoids are plotted at 50% probability.

Table 1. Bond lengths [Å] and angles [°] for $PTA–BH_3$ (**1**).

P(1)–C(2)	1.815(9)
P(1)–C(1)	1.830(12)
(B)N(1)–C	1.505(11)[a]
N(1)–B(1)	1.58(2)
N(2)–C	1.458(9)[b]
C(2)–P(1)–C(1)	95.0(4)
C(1)–N(1)–C(3)	109.3(6)
C–N(1)–B(1)	111.2(12), 110.0(7)
C–N(2)–C	108.0(8)–110.6(8)
N(1)–C(1)–P(1)	116.1(8)
N(2)–C(2)–P(1)	117.2(6)

[a] Average of two similar distances. [b] Average of three similar distances.

Table 2. Comparison of the bond lengths [Å] and angles [°] obtained from X-ray crystallography for **1**, **2**, PTA, and O=PTA.

	PTA[21,22]	$PTA–BH_3$ (**1**)	O=PTA[21,22]	O=PTA–BH_3 (**2**)
P–C	1.856	1.815(9), 1.830(12)	1.817	1.810 0(17)–1.8192(16)
N–C(N)	1.464	1.458(9), 1.464(9)	1.465	1.447(2), 1.468(2)
(B)N–C(N)	–	1.505(11)	–	1.5162(19), 1.5145(19)
N–C(P)	1.461	1.454(9), 1.504(13)	1.472	1.485(2),[a] 1.5011(18)
N–B	–	1.58(2)	–	1.616(2)
P=O	–	–	1.476	1.4903(11)
B–N–C	–	110.0(7), 111.2(12)	–	109.51(12),[a] 111.22(12)
C–P–C	96.07	95.0(4), 95.9(6)	100.18	100.42(7),[a] 101.95(8)
C–N–C	108.30	106.8(9)–110.6(8)	108.61	107.39(12)–113.15(12)
N–C–P	114.06	117.2(6), 116.1(8)	110.21	108.73(10),[a] 111.8(1)
C–P–O	–	–	117.66	114.08(7)–119.33(7)

[a] Average of two similar values.

in which one nitrogen atom of PTA has been protonated or alkylated.[20] Table 2 compares the bond lengths and angles of **1** with PTA and other PTA complexes.

Structure of O=PTA–BH_3 (2)

A thermal ellipsoid representation of complex **2** is depicted in Figure 3, along with the atomic numbering scheme. Selected bond lengths and angles may be found in Table 3. The P–O bond length in **2** [1.4903(11) Å] is slightly longer than found in O=PTA (P–O = 1.476 Å).[21,22] Noteworthy is that the B–N bond length in **2** [1.616(2) Å] is slightly longer than the B–N distance in **1** [1.58(2) Å], presumably due to the more positive nature of the formally P^V oxidation state of the phosphorus. Comparison of bond lengths and angles in **2** with O=PTA may be found in Table 2.

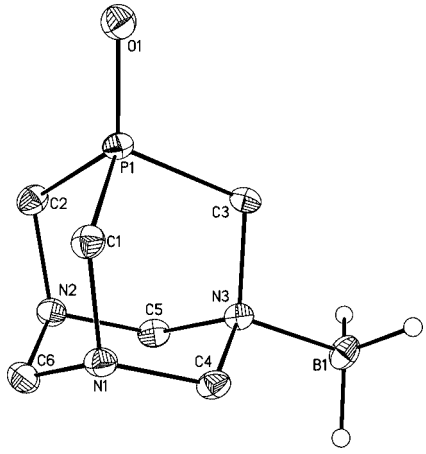

Figure 3. Thermal ellipsoid plot of O=PTA–BH_3 showing the atomic numbering scheme; hydrogen atoms have been omitted for clarity; thermal ellipsoids are plotted at 50% probability.

Table 3. Selected bond lengths [Å] and angles [°] for O=PTA–BH_3 (**2**).

P(1)–O(1)	1.4903(11)
P(1)–C	1.8100(17)–1.8192(16)
(B)N(3)–C	1.5011(18)–1.5162(19)
N(3)–B(1)	1.616(2)
N–C	1.447(2)–1.4879(19)
O–P(1)–C	114.07(7)–119.33(7)
C–P(1)–C	100.21(7)–101.95(8)
C–N(1)–C	109.35(12)–113.15(12)
C–N(2)–C	109.46(12)–112.87(12)
C–N(3)–C	107.39(12)–109.58(11)
C–N(3)–B(1)	109.46(12)–111.22(12)
N(3)–C(3)–P(1)	111.80(10)
N(1)–C(1)–P, N(2)–C(2)–P	108.88(10), 108.57(11)
N–C–N	113.52(12)–113.69(12)

Theoretical Calculations

In an attempt to gain insight into the reactivity differences between the nitrogen and phosphorus sites of PTA, calculations were performed modeling the alkylation and BH_3 addition to PTA. Density Functional Theory (DFT) calculations (B3LYP/LANL2DZ) were performed on **1**, **1-P**, PTA, PTA-Me, and Me-PTA as described in the experimental section. From these calculations we predict an energy difference of 53.6 kJ/mol between **1** and **1-P**, with **1** being the more stable isomer. This is consistent with calculations comparing the alkylation of PTA at the nitrogen atom (PTA-Me) or phosphorus (Me-PTA), which predict that nitrogen is the preferred site of alkylation by ca. 39.1 kJ/mol. These results are in agreement with those obtained by Darensbourg et al.[10] Table 4 contains comparisons of calculated geometries for **1**, **1-P**, **2**, PTA, and O=PTA. The bond lengths and angles in Table 4 correspond well that those found in the crystal structures of **1**, **2**, PTA, and O=PTA.

Reactivity of 1 and 2

Complexes of **1** and **2** are susceptible to hydrolytic cleavage of the boron–nitrogen bond in both the solid state and in solution. BH_3 may also be cleanly and easily removed from **1** or **2** by addition of excess diazobicyclooctane (DABCO) to an acetone solution of **1** or **2** at 50° C. One of the unusual features of **1** is that the phosphorus is now much more vulnerable to oxidation than PTA, $PTA(H)^+$, or $PTA(Me)^+$. Solids of PTA–BH_3 were stable in air for weeks, whereas solutions of PTA–BH_3 show signs of oxidation to O=PTA–BH_3 over the course of days, Scheme 3. In contrast, PTA, $PTAH^+$, and $PTAMe^+$ are indefinitely stable towards air oxidation in the solid state or solution. Both **1** and **2** must be stored under dry conditions, and **1** must be stored under nitrogen to prevent oxidation.

Table 4. DFT[a] calculated bond lengths and angles for **1**, **2**, PTA and O=PTA.

	PTA–BH_3[N] (**1**)	H_3B–PTA (**1-P**)[b]	O=PTA–BH_3 (**2**)	PTA	O=PTA
P–B	–	2.013	–	–	–
P–C	1.946, 1.929	1.927	1.914, 1.903	1.955	1.919
N–C(N)	1.465, 1.488, 1.540	1.493	1.466, 1.490, 1.542	1.492	1.494
N–C(P)	1.483, 1.519	1.483	1.486, 1.518	1.484	1.488
N–B	1.652	–	1.660	–	–
B–P–C	–	120.2	–	–	–
B–N–C	109.5, 109.6	–	109.5	–	–
C–P–C	94.1, 94.6	96.8	98.4, 98.5	93.8	98.0
P=O	–	–	1.610	–	1.614

[a] B3LYP/Lanl2dz. [b] BH_3 is phosphorus bound.

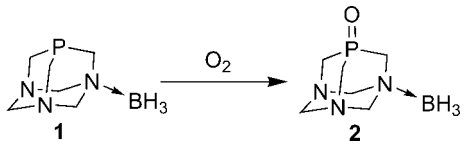

Scheme 3.

Addition of BH_3 appears to activate the phosphorus to alkylation as well as oxidation; addition of methyl iodide to PTA–BH_3 results in the formation of ca. 20% of the phosphorus-methylated product (Me-PTA) and ca. 80% of the nitrogen-methylated product (PTA-Me). Compared to the alkylation of PTA with MeI, which results in >95% PTA-Me and <5% Me-PTA the phosphorus in **1** is activated with respect to alkylation. This may open up new synthetic pathways towards high-yield synthesis of phosphorus-alkylated PTA compounds important in the further development of the chemistry of PTA and PTA derivatives. Currently phosphorus-alkylated PTA is synthesized by first alkylating $P(CH_2OH)_3$ followed by reaction with NH_4OAc and formaldehyde (Scheme 1).[12,13]

Synthesis of $[CpRu(PTA)_2Cl(Ph_3B_3O_3)]_n \cdot 1/2CH_2Cl_2$

We have previously reported the solid-state structure of $CpRu(PTA)_2Cl$.[4] In an attempt to access the cationic $CpRu(PTA)_2S^+$ complexes (where S = solvent; CH_3CN, H_2O), recently described,[23] we reacted $NaBPh_4$ with $CpRu(PTA)_2Cl$ in the presence of 1-propanol. Instead of the desired product, $[CpRu(PTA)_2S][BPh_4]$, we obtained crystals of the polymeric complex $[CpRu(PTA)_2Cl(Ph_3B_3O_3)]_n \cdot 3CH_2Cl_2$ in low yield (< 10%). The yield from this reaction is very low; the product is likely obtained due to small amounts of $Ph_3B_3O_3$ impurities in the $NaBPh_4$, or from adventitious water reacting with the tetraphenylborate anion generating triphenylboroxine. This complex was obtained in moderate yields (48%) by reaction of $CpRu(PTA)_2Cl$ with three equivalents of phenylboronic acid in dichloromethane, which affords large orange crystals of $[CpRu(PTA)_2Cl(Ph_3B_3O_3)]_n \cdot 1/2CH_2Cl_2$ (**3**). The polymer forms as a result of the cyclocondensation of phenylboronic acid, to triphenylboroxine, followed by formation of a Lewis acid–base adduct with the PTA ligands of $CpRu(PTA)_2Cl$ (Scheme 4); similar to the PTA–BH_3 complexes described above. Adducts of boroxines with amines have been reported;[24–30] however, compound **3** is the first involving PTA. Perzzuni et al. have described elsewhere the first heterobimetallic complex in which PTA exhibits both P and N coordination. In this case, $CpRu(PTA)_2Cl$ was treated with AgOTf leading to a polymeric structure in which PTA is bound to both ruthenium (by phosphorus) and silver (by nitrogen).[9] Complex **3** and the complexes described by Peruzzini are the only verifiable examples of PTA complexes in which the nitrogen sites of PTA are involved in dative bonding to another atom. It is now apparent that the nitrogen sites of PTA may be far from benign in the chemistry of PTA complexes. Unlike the water-soluble organometallic polymers of Peruzzini et al.,[9] compound **3** does not appear to remain polymeric in aqueous solution, presumably due to ring-cleavage hydrolysis of the coordinated $Ph_3B_3O_3$.

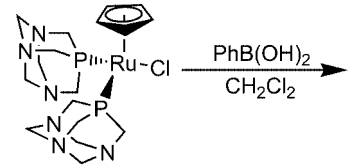

$[CpRu(PTA)_2Cl(Ph_3B_3O_3)]_n + 3n\ H_2O$

3

Scheme 4.

The ^{31}P NMR of the polymeric **3** in dichloromethane exhibits a broad singlet at –21.9 ppm, relative to the ^{31}P NMR chemical shift of –25.6 ppm for the parent $CpRu(PTA)_2Cl$. The ^1H NMR spectrum of **3**, in CD_2Cl_2, contains a sharp resonance attributed to the Cp protons at δ = 4.59 ppm an upfield shift of 0.16 ppm, relative to $CpRu(PTA)_2Cl$, indicating shielding of the protons by the phenyl groups of the boroxine as confirmed by the crystal structure. The NCH_2N protons of the PTA ligands in **3** exhibit an AB pattern centered at δ = 4.53 ppm ($^2J_{(HAHB)}$ = 13 Hz). The PCH_2N protons of the PTA ligands also exhibit an AB pattern centered at δ = 3.98 ppm ($^2J_{(HAHB)}$ = 15 Hz). The PTA protons are shifted downfield due to the deshielding effect of the N–B bonding. Two distinct resonances for the phenyl rings of the boroxine are observed, 8.07 ppm (5 H) and 7.5 ppm (10 H), indicating two different environments for the phenyl rings. ^{11}B NMR spectroscopy of **3** in acetone reveals two different boron environments with ^{11}B chemical shifts of 29.3 and 21.3 ppm indicative of unbound and bound boron nuclei, respectively.[31] This suggests that **3** remains polymeric in acetone with two of the boron atoms of triphenylboroxine coordinated to a PTA and remaining boron uncoordinated.

Structure of $[CpRu(PTA)_2Cl(Ph_3B_3O_3)]_n \cdot 1/2CH_2Cl_2$

The solid-state structure of **3** was determined by X-ray crystallography. Large orange crystals suitable for X-ray diffraction were obtained by slow diffusion of hexanes into a concentrated solution of **3** in CH_2Cl_2. A thermal ellipsoid representation of complex **3** is depicted in Figure 4, along with the atomic numbering scheme. Selected bond lengths and angles may be found in Table 5. The structure consists of $CpRu(PTA)_2Cl$ molecules linked together in linear chains by $Ph_3B_3O_3$, cocrystallized with half a molecule of CH_2Cl_2. The polymeric structure is obtained through formation of a Lewis acid–base adduct from one nitrogen atom on each PTA to a boron atom of triphenylboroxin. Two of the three boron atoms in triphenylboroxin form N–B bonds, which affords a linear polymer, with the geometry about the coordinated boron sites significantly distorted

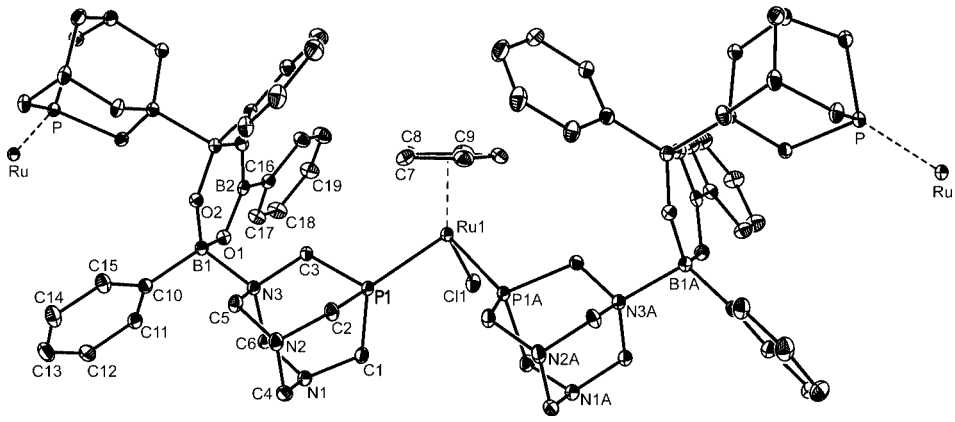

Figure 4. Thermal ellipsoid plot of **3** showing the atomic numbering scheme; hydrogen atoms have been omitted for clarity; thermal ellipsoids are plotted at 50% probability.

from planar towards tetrahedral with O–B–O angles of 115.8(2)° and N–B–C angles of 107.46(18)°. The boron atom, which is not coordinated to nitrogen is nearly planar with a O–B–O angle of 122.3(3)°. The B–N bond lengths are 1.737(3) Å, significantly longer than the N–B distances in compounds **1** and **2**, but comparable to other nitrogen-coordinated boroxin complexes which have B–N distances of 1.73–1.84 Å.[28–30] Comparison of the structure of **3** with the parent complex $CpRu(PTA)_2Cl$ and the diprotonated form $[CpRu(PTAH)_2Cl]^{2+}$, previously reported by us,[3,4] reveals that the core organometallic portion of **3** is largely unchanged, Table 6. The P–Ru–P angle is slightly less obtuse and the Ru–P bond lengths are elongated slightly (≈ 0.01 Å) in **3** vs. the other two complexes. The biggest change is in the (N)C–N distances within the PTA ligand, which have been utilized to determine when a PTA ligand has been protonated [on average the (N)C–N distance increases from ca. 1.46 to ca. 1.53 Å upon protonation].[20]

Table 5. Selected bond lengths [Å] and angles [°] for **3**.

Ru(1)–P(1)	2.2645(6)
Ru(1)–Cl(1)	2.4443(8)
N(1)–C	1.449(3)–1.470(4)
N(2)–C	1.445(3)–1.473(3)
N(3)–C	1.498(3)–1.513(3)
N(3)–B(1)	1.737(3)
O(1)–B(2)	1.368(3)
O–B(1)	1.439(3)[a]
B(1)–C(10)	1.625(4)
B(2)–C(16)	1.576(5)
P(1)–Ru(1)–P(1)#1	95.46(3)
P(1)–Ru(1)–Cl(1)	90.56(2)
C–N(3)–C	107.80(18)–109.66(18)
C–N(3)–B(1)	108.67(17)[a]
C(6)–N(3)–B(1)	113.27(16)
B(2)–O(1)–B(1)	121.1(2)
B(1)–O(2)–B(1)#2	123.4(3)
O(2)–B(1)–O(1)	115.8(2)
O–B(1)–C(10)	112.78(19)[a]
O–B(1)–N(3)	103.21(16), 103.57(19)
C(10)–B(1)–N(3)	107.46(18)
O(1)#2–B(2)–O(1)	122.3(3)
O(1)–B(2)–C(16)	118.83(16)

[a] Average of two similar values.

Table 6. Comparison of selected bond lengths [Å] and angles [°] for **3** with those reported for $CpRu(PTA)_2Cl$[4] and $[CpRu(PTAH)_2Cl](PF_6)_2$.[3]

	$CpRu(PTA)_2Cl$	$[CpRu(PTAH)_2Cl](PF_6)_2$	**3**
Ru–Cl	2.445(2)	2.455(2)	2.4443(8)
Ru–P(1)	2.258(3)	2.254(3)	2.2645(6)
Ru–P(2)	2.247(3)	2.257(3)	2.2645(6)[c]
$Ru–Cp_{cent}$	1.852	1.855	1.850
(N)C–N	1.460(2)[a]	1.448(11)[b]	1.472(3)[c]
(N)C–N(B/H)	–	1.516(12)[c]	1.512(3)[d]
P(1)–Ru–P(2)	96.85(5)	99.05(10)	95.46(3)
P(1)–Ru–Cl	91.61(7)	85.86(9)	90.56(2)
P(2)–Ru–Cl	86.46(7)	86.80(9)	90.56(2)[c]

[a] Average of 12 values. [b] Average of 8 values. [c] Average of 4 values. [d] Average of 2 values.

Conclusions

We have presented here the synthesis and characterization of three boron-coordinated PTA complexes. Peruzzini et al. published the first report of a PTA complex in which a metal is bound to a nitrogen of the PTA ligand.[9] Here we reported the second such complex, in which a nitrogen of a ruthenium-bound PTA serves as a Lewis base coordinating to the Lewis basic boron of triphenylboroxin. It should be noted that in both of these complexes the phosphorus atom of PTA is *already bound to a metal*. To the best of our knowledge, there are still no substantiated cases in the literature in which PTA serves only as a nitrogen donor ligand to a metal center. We reported here the closest example of such a structure; complex **1** represents the first coordination complex of PTA in which *only* the nitrogen of the PTA ligand is coordinated to another atom through a dative bond. Finally, it should be noted that the nitrogen sites of PTA may become involved in coordination chemistry and are not necessarily innocent bystanders. Complex **3** and the complexes previously reported by Peruzzini[9] may serve as a beginning for the use of PTA as a ligand in the building of extended structures, utilizing the ability of both the phosphorus and nitrogen sites of PTA to serve as Lewis bases.

Experimental Section

Materials and Methods: Unless otherwise noted all manipulations where performed on a double-manifold Schlenk vacuum line under nitrogen or in a nitrogen-filled glovebox. Nitrogen was purified by passing the gas through a column of molecular sieves (Lind 13X), calcium chloride, potassium hydroxide, and dryrite. Tetrakis-(hydroxymethyl)phosphonium chloride was obtained from Cytec and used as received. Ruthenium trichloride hydrate, D_2O, KOH, PPh_3, phenyl boronic acid, dicyclopentadiene, cyclooctadiene (COD), and BH_3–etherate were purchased from commercial sources and used as received. 1,3,5-Triaza-7-phosphaadamantane (PTA),[7,8] 1,3,5-triaza-7-phosphaadamatane oxide (O=PTA),[7] and $CpRu(PTA)_2Cl$[4,32] were prepared according to the literature procedures. Solvents were freshly distilled from standard drying reagents or dried with activated molecular sieves. Water was distilled and deoxygenated prior to use. NMR spectra were recorded with either a Varian Unity Plus 500 FT-MNR spectrometer, a GN 300 FT-NMR/Scorpio spectrometer, or a QE 300 FT-NMR/Aquarius spectrometer. Proton spectra were referenced to residual solvent relative to TMS with the exception of aqueous spectra, which were referenced to an external standard of sodium 2,2-dimethyl-2-silapentane-5-sulfonate (DSS). Phosphorus chemical shifts are relative to an external reference of 85% H_3PO_4 in D_2O with positive values downfield of the reference. ^{11}B chemical shifts are relative to an external reference of BF_3 in diethyl ether, with positive values downfield from the reference.

Synthesis of PTA–BH_3 (1): PTA (1.0 g, 6.4 mmol) was dissolved in a minimum amount of dichloromethane. The solution was then cooled in an ice bath and 1.1 equiv. of 1.0 M borane tetrahydrofuran complex was added via syringe (7 mL). The solution was stirred for 2 h, after which time the solvent was removed under vacuum leaving 1.01 g of a fine white solid (93% yield). ^1H NMR (300 MHz, [D_6]acetone, 25 °C): δ = 4.50–4.25 (m, 6 H, NCH_2N), 3.88–3.66 (m, 6 H, PCH_2N), 1.17 (q, $^1J_{BH}$ = 98 Hz, 3 H, BH_3) ppm. ^{11}B NMR (160 MHz, [D_6]acetone, 25 °C): δ = –10.8 (q, $^1J_{BH}$ = 98 Hz) ppm. $^{31}P\{^1H\}$ NMR (121 MHz, [D_6]acetone, 25 °C): δ = –88.4 (s) ppm. IR (KBr): $\tilde{\nu} = \upsilon_{(BH)}$: 2365 (s), 2312 (m), 2263 (m) cm^{-1}; $\upsilon_{(BN)}$: 1174 (s) cm^{-1}. IR (CH_2Cl_2): $\tilde{\nu} = \upsilon_{(BH)}$: 2370 (s), 2305 (m), 2271 (m) cm^{-1}; $\upsilon_{(BN)}$: 1172 (s) cm^{-1}. $C_6H_{15}BN_3P$: calcd. C 42.15, H 8.84, N 24.57; found C 42.20, H 8.90, N 25.02. X-ray quality crystals were grown by slow diffusion of hexanes into a concentrated THF solution of **1**, yielding colorless needles over the course of a week. A crystal suitable for X-ray diffraction was selected and mounted under oil on a glass fiber. Crystallographic data and data collecting parameters are listed in Table 7.

Synthesis of O=PTA–BH_3 (2): The borane complex of PTA oxide (O=PTA) was synthesized in a manner analogous to the PTA–borane complex described above. PTA=O (50 mg, 0.29 mmol) was dissolved in CH_2Cl_2 (20 mL) and BH_3–THF (1.0 mL, 1.0 M) was added at room temperature with stirring. The resultant solution turned cloudy and was stirred for an additional 1 h, after which time the product was collected by filtration. O=PTA–BH_3 was obtained as a fine white powder in 37% yield (20 mg). ^1H NMR (300 MHz, [D_6]acetone, 25 °C): δ = 4.5–3.8 (m, PTA), 1.47 (q, $^1J_{BH}$ = 95 Hz, BH_3) ppm. ^{11}B NMR (160 MHz, [D_6]acetone, 25 °C): δ = –12.2 (q, $^1J_{BH}$ = 95 Hz) ppm. $^{31}P\{^1H\}$ NMR (121 MHz, [D_6]-acetone, 25 °C): δ = –9.8 ppm. IR (KBr): $\tilde{\nu} = \upsilon_{(BH)}$: 2389 (s), 2325 (m), 2283 (m) cm^{-1}. $C_6H_{15}BN_3OP$: calcd. C 38.54, H 8.09, N 22.47; found C 38.92, H 8.51, N 22.56. Colorless X-ray quality crystals were obtained after approximately one week by layering a dilute solution of **2** in THF with hexane. A crystal suitable for X-ray diffraction was selected and mounted under oil on a glass fiber. Crystallographic data and data collecting parameters are listed in Table 7.

Synthesis of $[CpRu(PTA)_2Cl(Ph_3B_3O_3)]_n \cdot 1/2CH_2Cl_2$ (3): A Schlenk flask was charged with $CpRu(PTA)_2Cl$ (50 mg, 0.097 mmol) and

Table 7. Crystal data and structure refinement for **1**, **2**, and **3**.

	PTA–BH_3 (**1**)	O=PTA–BH_3 (**2**)	$[CpRu(PTA)_2Cl(Ph_3B_3O_3)]_n$ (**3**)
Empirical formula	$C_6H_{15}BN_3P$	$C_6H_{15}BN_3OP$	$[(C_5H_5)Ru(C_6H_{12}N_3)_2Cl(Ph_3B_3O_3)]\cdot 1/2CH_2Cl_2$
Formula mass	170.99	186.99	875.11
T (K)	100(2) K	100(2) K	100(2) K
Wavelength [Å]	0.71073 Å	0.71073 Å	0.71073 Å
Crystal system	monoclinic	monoclinic	orthorhombic
Space group	*Cm*	*P*21/*n*	*Ima*2
a [Å]	7.571(4)	6.1903(5)	22.9789(12)
b [Å]	9.244(4)	11.3929(9)	15.2606(8)
c [Å]	6.758(3)	12.7715(9)	11.4219(6)
α (°)	90	90	90
β [°]	114.900(10)	93.339(2)	90
γ [°]	90	90	90
Volume [$Å^3$]	429.0(3)	899.19(12)	4005.3(4)
Z	2	4	4
$D_{calcd.}$ [mg/m^3]	1.324	1.381	1.451
Abs. coefficient [mm^{-1}]	0.258	0.261	0.648
Crystal size [mm]	0.28 × 0.03 × 0.03	0.22 × 0.01 × 0.01	0.775×0.18×0.16
θ range for data collection	3.32 to 22.48°	2.40 to 27.50°	1.60 to 32.26°
Index ranges	$-8 \le h \le 8$, $-9 \le k \le 9$, $-7 \le l \le 7$	$-8 \le h \le 8$, $-14 \le k \le 14$, $-16 \le l \le 16$	$-34 \le h \le 34$, $-22 \le k \le 22$, $-17 \le l \le 17$
Reflections collected	1360	10013	26436
Independent reflections	598 [R(int) = 0.1467]	2048 [R(int) = 0.0396]	7202 [R(int) = 0.0228]
Absorption correction	SADABS	SADABS	SADABS
Data/restraints/parameters	598/2/65	2048/0/169	7202/1/261
Goodness-of-fit on F_2	0.812	1.026	1.167
Final R indices [$I > 2\sigma(I)$]	R_1 = 0.0689, wR_2 = 0.1007	R_1 = 0.0380, wR_2 = 0.0978	R_1 = 0.0341, wR_2 = 0.1106
R indices (all data)	R_1 = 0.1247, wR_2 = 0.1138	R_1 = 0.0470, wR_2 = 0.1028	R_1 = 0.0344, wR_2 = 0.1109

$PhB(OH)_2$ (36 mg, 0.295 mmol); the solids were dissolved in a minimum volume (≈ 5 mL) of dichloromethane and stirred under nitrogen for 10 h. Addition of hexanes afforded 38 mg (48%) $[CpRu(PTA)_2Cl(Ph_3B_3O_3)]_n$·1/2 CH_2Cl_2 (**3**) as orange crystals. ^1H NMR (300 MHz, CD_2Cl_2, 25 °C): δ = 8.0–8.1 (m, 5 H, ArH), 7.35–7.45 (m, 10 H, ArH), 4.4–4.6 (AB spin system, $^2J_{(HAHB)}$ = 13 Hz, 17 H, Cp, NCH_2N), 3.9–4.1 (AB spin system, $^2J_{(HAHB)}$ = 15 Hz, 12 H, PCH_2N) ppm. ^{11}B NMR (160 MHz, [D$_6$]acetone, 25 °C): δ = 29.3 (s, $B_{uncoordinated}$), 21.3 (br. s, *B*–N) ppm. $^{31}P\{^1H\}$ NMR (121 MHz, CD_2Cl_2, 25 °C): δ = –21.9 (br. s, Ru–PTA) ppm. IR (KBr): $\tilde{\nu} = \upsilon_{(BO)}$: 1387, 1344, 1310 cm^{-1}. $C_{36}H_{45}B_3Cl_2N_6O_3P_2Ru$: calcd. C 49.35, H 5.18, N 9.59; found C 50.51, H 5.14, N 9.42. Dark orange X-ray quality crystals were grown by slow diffusion of hexanes into a CH_2Cl_2 solution of **3** over the course of 4 days. A crystal suitable for X-ray diffraction was selected and mounted under oil on a glass fiber. Crystallographic data and data collecting parameters are listed in Table 7.

Computational Details: Theoretical calculations were performed in an attempt to obtain insight into the differential reactivity of the phosphorus and nitrogen nuclei of PTA. All calculations were run on a Beowulf cluster of 16 dual processor computers operating under Linux. Theoretical calculations were performed using the Gaussian 03 program package employing the LANL2DZ basis set of Wadt and Hay[33,34] as implemented in Gaussian 03.[35] Density functional (DFT) calculations were carried out on all complexes using Becke's three-parameter hybrid method[36] coupled to the correlation functional of Lee, Yang, and Parr (B3LYP).[37] Frequency calculations were performed on all optimized structures in order to establish the nature of the extrema and to calculate values for ΔH and ΔG. Full geometry optimizations were performed on **1**, **1-P**, PTA, PTA-Me, and Me-PTA starting from the crystal structures of each compound.

CCDC-288665 to -288667 contain the supplementary crystallographic data for this paper. These data can be obtained free of charge from The Cambridge Crystallographic Data Centre via www.ccdc.cam.ac.uk/data_request/cif.

Acknowledgments

The authors would like to thank Brady Janes and Lauren Volz for their help on this project. PWG would like to thank the NSF-EPSCoR program (EPS-0132556) for a summer fellowship and UNR for an undergraduate research award supporting this project. We thank Cytec for the generous gift of $P(CH_2OH)_4Cl$. Financial support from the National Science Foundation is acknowledged for funding for the X-ray diffractometer (CHE-0226402).

[1] See for example: J. Andrieu, J.-M. Camus, P. Richard, R. Poli, L. Gonsalvi, F. Vizza, M. Peruzzini, *Eur. J. Inorg. Chem.* **2006**, 51–61; J. Andrieu, J.-M. Camus, P. Richard, R. Poli, L. Gonsalvi, F. Vizza, M. Peruzzini, *Eur. J. Inorg. Chem.* **2006**, 51–61; J. Andrieu, J.-M. Camus, C. Balan, R. Poli, *Eur. J. Inorg. Chem.* **2006**, 62–68; J. Andrieu, P. Richard, J.-M. Camus, R. Poli, *Inorg. Chem.* **2002**, *41*, 3876–3885; J. Andrieu, J.-M. Camus, J. Dietz, P. Richard, R. Poli, *Inorg. Chem.* **2001**, *40*, 1597–1605; C. Müller, C. N. Iverson, R. J. Lachicotte, W. D. Jones, *J. Am. Chem. Soc.* **2001**, *123*, 9718–9719; P. Espinet, K. Soulantica, *Coord. Chem. Rev.* **1999**, *193–195*, 499–556; F. Stöhr, D. Sturmayr, G. Kickelbick, U. Schubert, *Eur. J. Inorg. Chem.* **2002**, 2305–2311; P. Molina, A. Arques, A. García, M. C. Ramírez de Arellano, *Eur. J. Inorg. Chem.* **1998**, 1359–1368; G. R. Newkome, *Chem. Rev.* **1993**, *93*, 2067–2089; D. B. Grotjahn, D. A. Lev, *J. Am. Chem. Soc.* **2004**, *126*, 12232–12233.

[2] See for example: W. J. Knebel, R. J. Angelici, O. A. Gansow, D. J. Darensbourg, *J. Organomet. Chem.* **1974**, *66*, C11–C13; W. J. Knebel, R. J. Angelici, *Inorg. Chem.* **1974**, *13*, 632–637; W. J. Knebel, R. J. Angelici, *Inorg. Chem.* **1974**, *13*, 627–631; T. B. Rauchfuss, D. M. Roundhill, *J. Am. Chem. Soc.* **1974**, *96*, 3098–3105; G. P. C. M. Dekker, A. Buijs, C. J. Elsevier, K. Vrieze, P. W. N. M. van Leeuwen, W. J. J. Smeets, A. L. Spek, Y. F. Yang, C. H. Stam, *Organometallics* **1992**, *11*, 1937–1948.

[3] C. A. Mebi, B. J. Frost, *Organometallics* **2005**, *24*, 2339–2346.

[4] B. J. Frost, C. A. Mebi, *Organometallics* **2004**, *23*, 5317–5323.

[5] B. J. Frost, S. B. Miller, K. O. Rove, D. M. Pearson, J. D. Korinek, J. L. Harkreader, C. A. Mebi, J. Shearer, *Inorg. Chem. Acta* **2006**, *359*, 283–288.

[6] A. D. Phillips, L. Gonsalvi, A. Romerosa, F. Vizza, M. Peruzzini, *Coord. Chem. Rev.* **2004**, *248*, 955–993 and references within.

[7] D. J. Daigle, *Inorg. Synth.* **1998**, *32*, 40–45.

[8] D. J. Daigle, A. B. Pepperman Jr, S. L. Vail, *J. Heterocycl. Chem.* **1974**, *11*, 407–408.

[9] C. Lidrissi, A. Romerosa, M. Saoud, M. Serrano-Ruiz, L. Gonsalvi, M. Peruzzini, *Angew. Chem. Int. Ed.* **2005**, *44*, 2568–2572.

[10] D. J. Darensbourg, J. C. Yarbrough, S. J. Lewis, *Organometallics* **2003**, *22*, 2050–2056.

[11] D. J. Daigle, A. B. Pepperman Jr, *J. Heterocycl. Chem.* **1975**, *12*, 579–580.

[12] E. Fluck, H. J. Weissgraeber, *Chem.-Ztg.* **1977**, *101*, 304–304.

[13] B. Assmann, K. Angermaier, M. Paul, J. Riede, H. Schmidbaur, *Chem. Ber.* **1995**, *128*, 891–900.

[14] R. W. Rudolph, C. W. Schultz, *J. Am. Chem. Soc.* **1971**, *93*, 6821–6822.

[15] A. H. Cowley, M. C. Damasco, *J. Am. Chem. Soc.* **1971**, *93*, 6815–6820.

[16] L. M. R. Martinez-Aguilera, G. Cadenas-Pliego, R. Contreras, A. Flores-Parra, *Tetrahedron: Asymmetry* **1995**, *6*, 1585–1592.

[17] A. Flores-Parra, S. A. Sánchez-Ruíz, C. Guadarrama-Pérez, *Eur. J. Inorg. Chem.* **1999**, 2063–2068.

[18] A. J. Arduengo, US Patent WO9003990, 1990.

[19] F. Hanic, V. Subrtova, *Acta Crystallogr., Sect. B* **1969**, *25*, 405–409.

[20] D. J. Darensbourg, T. J. Decuir, J. H. Reibenspies, in *Aqueous Organometallic Chemistry and Catalysis* (Eds.: I. T. Horvath, F. Joo); High Technology; Kluwer: Dordrecht, The Netherlands, **1995**; pp. 61–80.

[21] K. H. Jogun, J. J. Stezowski, E. Fluck, J. Weidlein, *Phosphorus Sulfur* **1978**, *4*, 199–204.

[22] R. E. Marsh, M. Kapon, S. Hu, F. H. Herbstein, *Acta Crystallogr., Sect. B* **2002**, *58*, 62–77.

[23] S. Bolano, L. Gonsalvi, F. Zanobini, F. Vizza, V. Bertolasi, A. Romerosa, M. Peruzzini, *J. Mol. Cat. A* **2004**, *224*, 61–70.

[24] M. A. Beckett, D. S. Brassington, P. Owen, M. B. Hursthouse, M. E. Light, K. M. A. Malik, K. S. Varma, *J. Organomet. Chem.* **1999**, *585*, 7–11.

[25] M. A. Beckett, D. E. Hibbs, M. B. Hursthouse, P. Owen, K. M. A. Malik, K. S. Varma, *Main Group Chem.* **1998**, *2*, 251–258.

[26] M. A. Beckett, G. C. Strickland, K. S. Varma, D. E. Hibbs, M. B. Hursthouse, K. M. A. Malik, *J. Organomet. Chem.* **1997**, *535*, 33–41.

[27] M. A. Beckett, G. C. Strickland, K. S. Varma, D. E. Hibbs, M. B. Hursthouse, K. M. A. Malik, *Polyhedron* **1995**, *14*, 2623–2630.

[28] M. Yalpani, R. Boese, *Chem. Ber.* **1983**, *116*, 3347–3358.

[29] J. C. Norrild, I. Sotofte, *J. Chem. Soc., Perkin Trans. 2* **2002**, 303–311.

[30] L. I. Bosch, M. F. Mahon, T. D. James, *Tetrahedron Lett.* **2004**, *45*, 2859–2862.

[31] W. Kliegel, K. Drückler, B. O. Patrick, S. J. Rettig, J. Trotter, *Acta Crystallogr., Sect. E* **2002**, *58*, o831–o833.

[32] D. N. Akbayeva, L. Gonsalvi, W. Oberhauser, M. Peruzzini, F. Vizza, P. Brueggeller, A. Romerosa, G. Sava, A. Bergamo, *Chem. Commun.* **2003**, 264–265.
[33] W. R. Wadt, P. J. Hay, *J. Chem. Phys.* **1985**, *82*, 284–298.
[34] P. J. Hay, W. R. Wadt, *J. Chem. Phys.* **1985**, *82*, 270–283.
[35] M. J. Frisch, G. W. Trucks, H. B. Schlegel, G. E. Scuseria, M. A. Robb, J. R. Cheeseman, J. A. Montgomery Jr, T. Vreven,K. N. Kudin, J. C. Burant, J. M. Millam, S. S. Iyengar, J. Tomasi, V. Barone, B. Mennucci, M. Cossi, G. Scalmani, N. Rega, G. A. Petersson, H. Nakatsuji, M. Hada, M. Ehara, K. Toyota, R. Fukuda, J. Hasegawa, M. Ishida, T. Nakajima, Y. Honda, O. Kitao, H. Nakai, M. Klene, X. Li, J. E. Knox, H. P. Hratchian, J. B. Cross, C. Adamo, J. Jaramillo, R. Gomperts, R. E. Stratmann, O. Yazyev, A. J. Austin, R. Cammi, C. Pomelli, J. W. Ochterski, P. Y. Ayala, K. Morokuma, G. A. Voth, P. Salvador, J. J. Dannenberg, V. G. Zakrzewski, S. Dapprich, A. D. Daniels, M. C. Strain, O. Farkas, D. K. Malick, A. D. Rabuck, K. Raghavachari, J. B. Foresman, J. V. Ortiz, Q. Cui, A. G. Baboul, S. Clifford, J. Cioslowski, B. B. Stefanov, G. Liu, A. Liashenko, P. Piskorz, I. Komaromi, R. L. Martin, D. J. Fox, T. Keith, M. A. Al-Laham, C. Y. Peng, A. Nanayakkara, M. Challacombe, P. M. W. Gill, B. Johnson,W. Chen, M. W. Wong, C. Gonzalez, J. A. Pople, *Gaussian 03, Revision B.02*, Gaussian, Inc.: Pittsburgh, PA, **2003**.
[36] A. D. Becke, *Phys. Rev. A* **1988**, *38*, 3098–3100.
[37] C. Lee, W. Yang, R. G. Parr, *Phys. Rev. B* **1988**, *37*, 785–789.
Received: November 15, 2005
Published Online: February 2, 2006

